IOSR Journal of Applied Chemistry (IOSR-JAC)
e-ISSN: 2278-5736.Volume 8, Issue 5 Ver. II (May. 2015), PP 13-21
www.iosrjournals.org

Effects of oil shale addition on the microstructure and mechanical properties of porous ceramics from Moroccan raw clay

A. Abourriche[1*], A. Benhammou[1], Y. El hafiane[1], Y. Abouliatim[1], L. Nibou[1], M. Oumam[2], H. Hannache[2,3], M. Birot[4] , A. Smith[5]

[1]*Laboratoire des Matériaux, Procédés, Environnement et Qualité, École Nationale des Sciences Appliquées, B.P. 63 46000 Safi, Morocco.*

[2]*Laboratoire des Matériaux Thermostructuraux, Faculté des Sciences Ben M'sik, B.P. 7955 Casablanca, Morocco.*

[3]*Center for Advanced Materials Université Mohammed VI Polytechnique, Lot 660 – hay Moulay Rachid 43150 Ben Guerir, Morocco.*

[4d]*Université de Bordeaux, Institut des Sciences Moléculaires, CNRS, UMR 5255, F-33400 Talence, France.*

[5]*Groupe d'Etude des Matériaux Hétérogènes GEMH, ENSCI, 47-73, Avenue Albert Thomas, 11 87065 Limoges Cedex, France*

Abstract: *Within the Moroccan natural resources valorization scheme, porous ceramics have been prepared from clay minerals and oil shale sintered between 1000 and 1100 °C. X-ray diffraction, differential thermal analysis and scanning electron microscopy were used to examine the structural and microstructural changes of the materials. Porosity and pore size distribution were measured using mercury intrusion porosimetry. The mechanical properties were investigated by three-point flexural and Brazilian tests, while the elastic properties were evaluated by ultrasonic non-destructive testing. When sintered at 1100 °C, ceramics prepared by mixing raw clay and oil shale are twice as porous as materials obtained from clay only (43.89 and 19.32 % respectively).*

Keywords*: Clay, Mechanical Properties, Oil Shale, Porous Ceramic.*

I. Introduction

Nowadays, technical ceramics are offering specific (physical, thermal, optical, electrical…) properties that allow providing new opportunities in the field of industrial development, and that open wide domains of applications and utilizations, particularly for porous ceramics, whose demand has become very important, especially as efficient filtration media [1–4]. A lot of research work [5–8] has been reported on their processes of production in order to develop new techniques to obtain high quality ceramics, while meeting the specifications imposed by the industrials.

There are numerous techniques for increasing porosity of ceramics, such as sintering methods using pore formers and/or partial sintering, or by introduction of additives [9–12]. Okada et al. [13] used organic fibers as the pore former to prepare porous mullite ceramics with unidirectionally oriented pores. They showed that the thin and thick lotus ceramics prepared had porosities of 47 and 49%, average pore radii of about 7.8 μm and gas permeabilities of 4.1×10^{-14} and 5.6×10^{-14} m^2, respectively. More recently, Li et al. [14] reported the effect of starch addition on microstructure and properties of highly porous alumina ceramics and their results revealed that the porosity was raised with increasing starch content from 0 to 30 vol%, which caused the decrease in thermal conductivity, whereas the compressive strength was maintained at a relatively high value. Feng et al. [15] investigated on using water and acetone as solvents to prepare mixed PVP–alumina powders for formation of porous alumina ceramics by dry pressing. They showed that the use of water resulted in a uniform pore structure compared to acetone-assisted ball milling and dry milling. In addition, the acetone-mixing PVP/alumina sample had the highest strength as well as Young's modulus, due to formation of cylindrical pore structure. Both porosity and pore morphology affected mechanical properties: the samples with cylindrical pores had the highest bending strength as well as Young's modulus as compared with those prepared without PVP at a similar porosity. Higher bending strength was obtained for the acetone-mixing alumina sample, and the deviation value of strength was higher compared to the water-mixing alumina sample.

[*]Corresponding author. Tel.: *00 212 64456721 Fax:* 0021224698012.
E-mail address: *krimabou@hotmail.com*

Generally, Industrial ceramic supports are prepared from expensive compounds, such as Al_2O_3, SiO_2, TiO_2 or SiC, but recently, considerable efforts have been accomplished to prepared ceramics from cheaper materials: e.g. cordierite and clay [16–19].

Within this context, we have carried out researches to explore the opportunity of producing porous ceramics from Moroccan abundant natural resources, i.e. clays and oil shales, in order to find new applications of the Moroccan oil shales [20–21]. The present work aimed to investigate whether oil shale behaved as an efficient additive to produce macroporous ceramics with significant porosity and to examine the mechanical properties. In this paper, we compare the experimental results obtained for materials prepared using clay only with those obtained for materials prepared by mixing clay and oil shale.

II. Experimental

2.1. Materials and methods

2.1.1 Raw materials

The clay raw material (CR) came from Safi, located on the West Coast of Morocco. This natural red clay is locally exploited mainly in the brick industry and artisanal pottery. The Moroccan oil shale (OS) was obtained from the Timahdit deposit, located in the Middle Atlas Mountai

2.1.2 Porous ceramic synthesis

The clay was homogenized using a rotary mixer for 1 h. Then the powder was uniaxially pressed at 8 MPa in a stainless steel die (D: 22 mm) for 10 min. The compacted pellets were sintered at selected temperatures using a heating rate of 10°C min^{-1} and a 2 h dwelling at the maximal temperature. Three samples were prepared using clay only: **sample 1** sintered at 1000 °C, **sample 2** sintered at 1050 °C and **sample 3** sintered at 1100 °C.

Mixtures of raw clay and oil shale (1:1 w/w) were prepared at room temperature by dry mixing. The mixtures were homogenized using a rotary mixer for 1 h. Then the powders were uniaxially pressed at 8 MPa in a stainless steel die (D: 22 mm) for 10 min. The compacted pellets were heated at 1000, 1050 and 1100 °C. Sintering was carried at selected temperatures using a heating rate of 10°C min^{-1} and a 2 h dwelling at the maximal temperature. Three samples were prepared under the conditions described above: **sample 4** sintered at 1000 °C, **sample 5** sintered at 1050 °C and **sample 6** sintered at 1100 °C.

2.1.3. Characterizations

Chemical analysis by X-ray fluorescence was performed on a BRPM-type fluorimeter. The powdered samples were mixed with a flux (calcium and magnesium borate), pressed as pellets, and then heated up to 1000 °C in an induction oven.

The porosity and pore size distribution were measured by mercury intrusion porosimetry (MIP) using a Micromeritics Autopore IV 9500 analyzer with the following parameters: T = 22 °C; sample mass = 600 mg; pressure range 0.002 to 220 MPa, mercury surface tension = 485 dyne•cm^{-1} and contact angle 130 °.

Scanning electron microscopy (SEM) micrographs were taken with a Hitachi TM-1000 microscope. Fragments of about 0.5 cm^2 cut from the corresponding samples were mounted on a carbon tab, which ensured a good conductivity. A thin layer of gold-palladium was sputtered prior to analysis.

The X-ray diffraction (XRD) patterns of the raw materials and the ceramics were obtained with a Siemens D500 instrument, using Cu K□ radiation (λ = 0.15405 nm) at 40 kV and 30 mA. The samples were tested in the range of 5–60 ° with a step of 0.02 °. Crystalline phases were identified by comparison with Powder Diffraction Files (PDF) standards from the International Center for Diffraction Data (ICDD).

The thermogravimetric and differential thermal analyses (DTA) were carried out under N56 high purity argon flow (40 ml·min^{-1}) with a Netzsch STA 409 apparatus. Samples of about 12 mg were heated from 50 to 950 °C at a heating rate of 5 °C·min^{-1}.

The three-point flexure test was performed at room temperature using a universal testing machine (Ametek Lloyd Instruments). The load was applied at the midpoint of the specimen and at a displacement rate of 0.1 mm·min^{-1} until fracture occurred. Thickness t, width w, and length of the specimens were 6, 9 and 60 mm, respectively. The flexural strength at failure σ_f determined from the theory of elasticity was calculated as follows [22]:

$$\sigma_f = \frac{3}{2}\frac{F L}{w t^2} \quad (1)$$

where F(N) is the load at fracture, and L is the distance between the two supports (50 mm).

The Brazilian test was performed at ambient temperature on cylindrical samples with a diameter D of 22 mm and a thickness h of 3 mm. The indirect tensile strength σ_t (MPa) was calculated by the following formula:

$$\sigma_T = \frac{F}{S} = \frac{2F}{\pi D h} \quad (2)$$

where F(N) is the applied load.

Elastic properties were determined by ultrasonic echography (Panametric Sofranel instrument) as a non-destructive testing. The tests were carried out on cylindrical specimens with a diameter of 32 mm and a thickness w of 3 mm. The velocity of sound V was calculated from the equation:

$$V = \frac{2w'}{t'} \quad (3)$$

where V, w', and t' are the velocity of sound, the thickness of the sample, and the time delay between two successive echoes, respectively.

Elastic properties such as the dynamic Young's modulus (E_D), shear modulus (G) and Poisson's ratio (ν) were evaluated according to the following formulas:

$$E_D = \rho . \frac{(3V_L^{\,2} - 4V_T^{\,2})}{(\frac{V_L^{\,2}}{V_T^{\,2}} - 1)} \quad (4)$$

$$G = \rho . V_T^{\,2} \quad (5)$$

$$\nu = \frac{E}{2.G} - 1 \quad (6)$$

where V_L and V_T are the longitudinal and transverse wave velocities ($m \cdot s^{-1}$) and □ the density of the sample ($g \cdot cm^{-3}$), respectively.

III. Results and discussion

3.1. Characterization of raw materials

Characterizations of clay and oil shale were made on grinded samples sieved at 60 µm.

XRD analyses were carried out on raw materials (Figure 1). The identification of the mineral phases was achieved by comparing the diffractograms obtained with the ASTM data [23]. The chemical composition of the oil shale rock and the red clay presented in

Table 1 lead to the following conclusions:

- The main components of shale rock and clay are silica SiO_2, alumina Al_2O_3 and lime CaO. These oxides represent 48.33 % and 74.17 % in mass of the shale and of the clay respectively. Besides, iron present in the clay explains its red color.
- Both materials contain flux such as alkalis (K_2O, Na_2O) and magnesia (MgO). Their proportions are around 7.88 % for the shale and 7.57 % for the clay.

Mass losses of oil shale and red clayat 1000 °C were obtained by TGA under inert atmosphere. The mass loss of oil shale (40.4%) corresponds to elimination of water, organic matter and CO_2 coming from the decomposition of carbonates. In the case of red clay, the mass loss (11.7%) is due to elimination of water only.

Table 1: Chemical compositions of oil shale rock and red clay (wt%)

	P_2O_5	MnO	K_2O	Na_2O	TiO_2	Fe_2O_3	Al_2O_3	SiO_2	MgO	CaO
Oil Shale rock	1.86	<0.01	1.24	<0.05	0.37	2.63	6.96	26.58	4.53	14.79
Red Clay	0.17	< DL	4.62	0.42	< DL	5.85	17.44	52.79	2.53	3.94

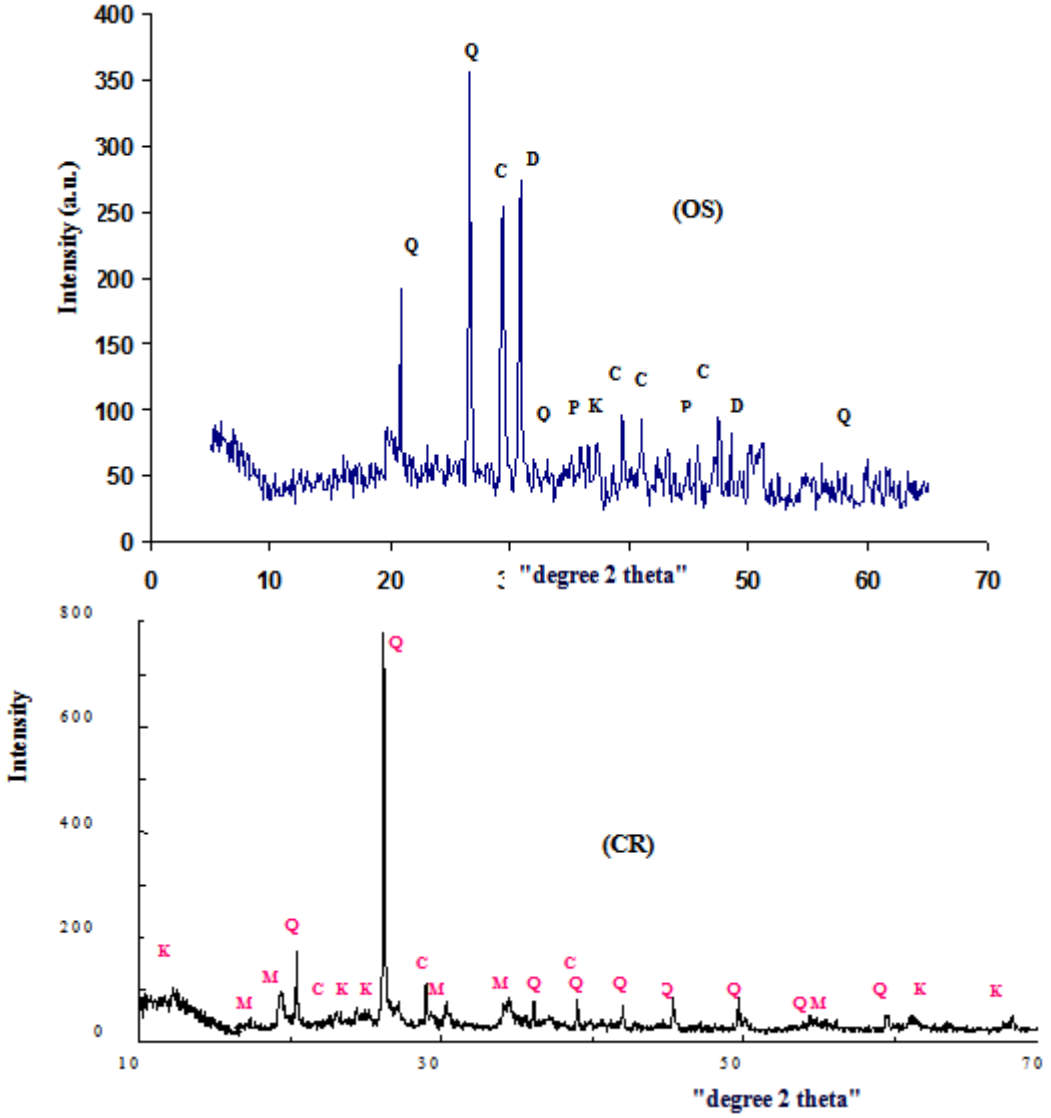

Figure 1: XRD of oil shale (OS) and red clay (RC) at 25 °C (K = kaolinite; M = muscovite; Q = quartz; C = calcite; P = pyrite; D = dolomite)

3.2. Characterization of the obtained materials

3.2.1 Materials prepared using clay only

As noted in the experimental part, three samples were prepared using clay only: **sample 1** sintered at 1000 °C, **sample 2** sintered at 1050 °C and **sample 3** sintered at 1100 °C.

The results of MIP analyses and the tensile strength values presented in

Table 2 show that the temperature has an effect on the porosity and the mechanical properties of the materials obtained from clay alone. Indeed, the porosity decreases and the tensile strength value increases with increasing temperature. Similar results were reported by Saffaj et al. [24] during the characterization of microfiltration and ultrafiltration membranes deposited on raw support prepared from Moroccan clay.

Table 2: Effect of sintering temperature on tensile strength and porosity for materials prepared from clay only

	Temperature (°C)	Porosity (%)	Apparent density ($g \cdot cm^{-3}$)	Bulk density ($g \cdot cm^{-3}$)	Tensile strength (MPa)
Sample 1	1000	28.31	2.70	1.93	20.8 ± 2.4
Sample 2	1050	27.83	2.68	1.93	19.1 ± 3.1
Sample 3	1100	19.32	2.53	2.04	24.1 ± 2.1

Figure 2 illustrates SEM micrographs of **samples 1–3**. The comparison of these SEM pictures shows that **sample 3**, sintered at 1100 °C, show less porous structure. This confirms the results obtained by MIP analyses.

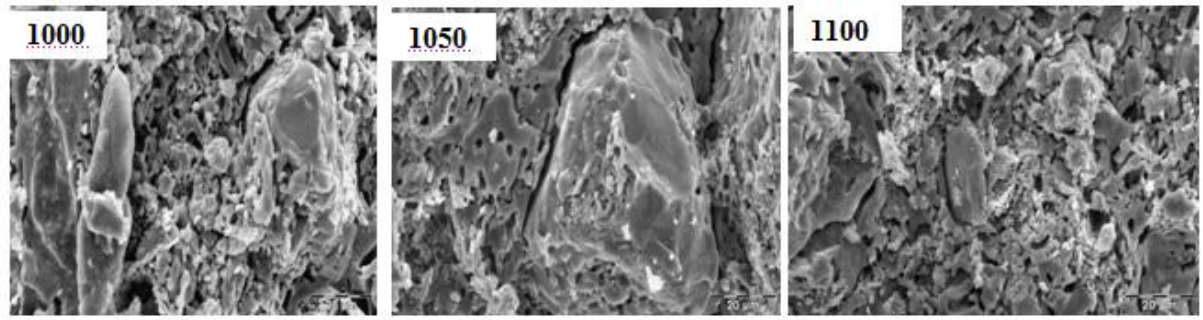

Figure 2: SEM micrographs of samples prepared from clay only

3.2.2 Materials prepared by dry mixing of raw clay and oil shale

First, in order to study the behavior of the mixture of raw clay and oil shale during heat treatment, an analysis was performed by DTA. The DTA plot (**Figure 3)** presents four areas: the first, between 60 °C and 130 °C, is due to elimination of water. The second (from 320 °C to 470 °C) is caused by the decomposition of the organic matter of the oil shale. The third, in the range 500–670 °C, is due to dehydroxylation of clay minerals. The fourth, in the range 750–870°C, corresponds to the decomposition of carbonates, essentially calcite and dolomite. In fact, it is admitted that dolomite $CaMg(CO_3)_2$ decomposes first between 700 and 800 °C to form MgO. In contrast, calcite $CaCO_3$ decomposes at higher temperature [25].

Next, to appreciate the potential of oil shale as an additive to produce porous ceramics, three samples were prepared under the conditions described in the experimental part: **sample 4** sintered at 1000 °C, **sample 5** sintered at 1050 °C and **sample 6** sintered at 1100 °C.

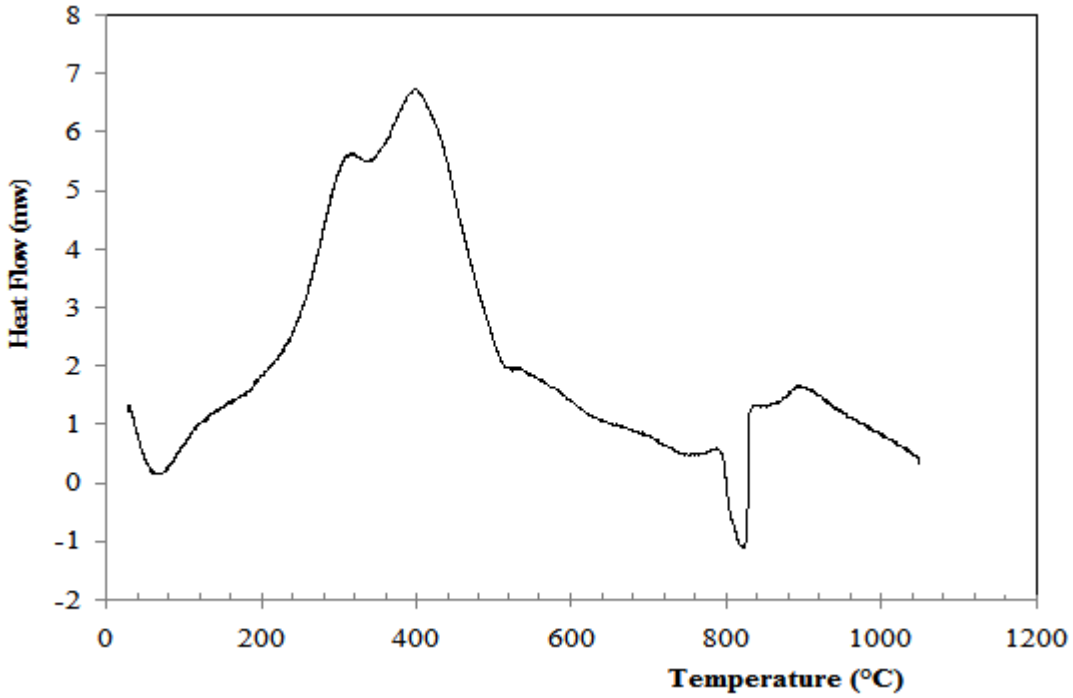

Figure 3: DTA plot of a 50:50 wt% oil shale/clay mixture

The results of MIP analyses are shown in Table 3. We note that the porosity almost doubled compared with the samples obtained using clay only (

Table 2). These results show that the use of oil shale as natural and less expensive pores forming agent can be an interesting alternative for the manufacture of porous ceramics. S**ample 6** sintered at 1100 °C having

the highest porosity. The increase in porosity with oil shale addition may be due mainly to the increase of CO_2 gas released from the thermal decomposition of both organic matter and carbonates.

Table 3: Effect of sintering temperature on densification and flexural strength for materials prepared by mixing clay and oil shales

	Temperature (°C)	Porosity (%)	Apparent density ($g \cdot cm^{-3}$)	Bulk density ($g \cdot cm^{-3}$)	Flexural strength (MPa)
Sample 4	1000	40.85	2.81	1.66	15.2 ± 0.9
Sample 5	1050	38.64	2.71	1.66	18.2 ± 2.7
Sample 6	1100	43.89	2.72	1.52	22.1 ± 2.1

The pore size distributions of the samples are shown in Figure The porous structure is uniform, all materials having almost 90% of the pores with diameter within the range 1.5–3 μm, which corresponds to macroporous ceramics.

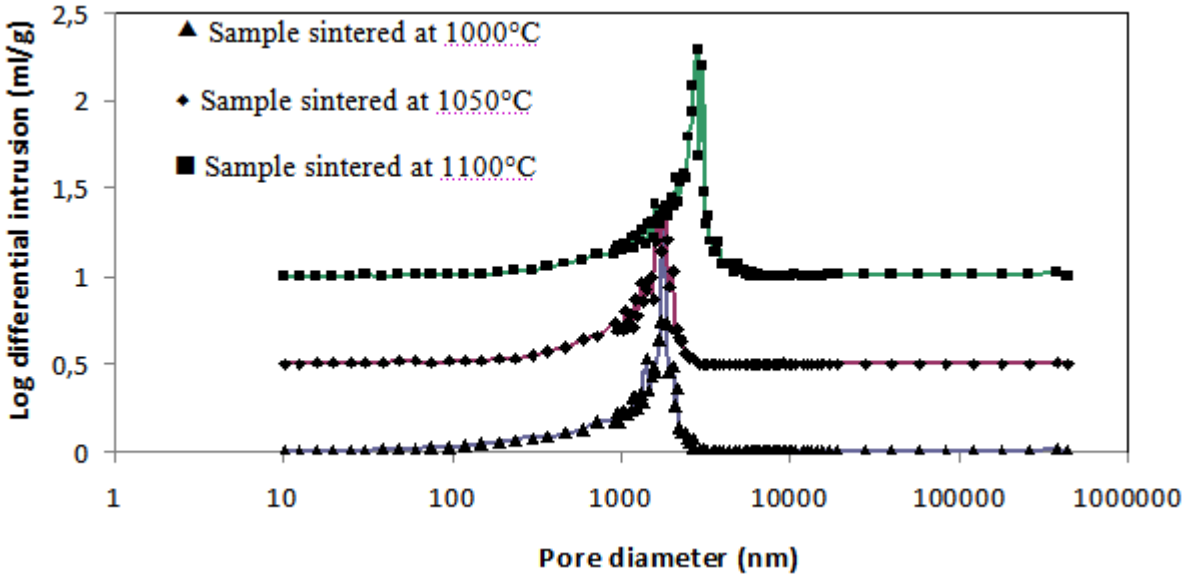

Figure 4: Pore size distribution of samples prepared by mixing clay and oil shales

Figure 5 illustrates SEM micrographs of the macroporous ceramics sintered at the three different temperatures. All the samples showed a surface with rough morphological structure. **Sample 6,** sintered at the highest temperature, shows highly porous structure compared to other samples, which corroborates the results of MIP analyses.

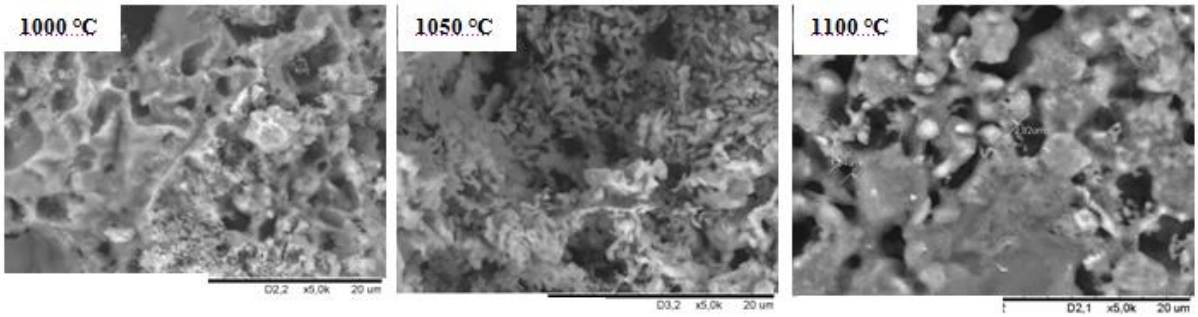

Figure 5: SEM micrographs of samples prepared by mixing clay and oil shales

The mechanical resistance test was performed using the three points bending strength to control the resistance of the samples fired at different temperatures. The mechanical strength reported in Table 3**Error! Reference source not found.** increases with increasing sintering temperature and reaches 22.1 ± 2.1 MPa at 1100 °C. This value is relatively lower than that of porous ceramic prepared from clay reported in previous works [19, 26]. The gradual improvement in mechanical properties observed when the temperature increases from 1000 to 1100 °C is linked possibly to the formation of mullite, phase known for its good mechanical properties [27–29].

Figure 6 shows load-deflection curve of **sample 6** sintered at 1100 °C. The load-displacement curve is similar to a linear behavior without apparition of the sudden failure. This confirms that the material is elastic and characterized by a uniform distribution of pores. It must be noted that all samples have the same curve.

The material obtained at a firing temperature of 1100 °C (**sample 6**) was selected to study its elastic properties and behavior during the diametral compression test (Brazilian test). The shape of the load-displacement curve in **Figure** 7 confirms the linear elastic and brittle behavior determined by the three point bending test. The load was first gradually increased and then increased linearly up to rupture. This is probably attributable to the compression of pores during loading. The tensile strength value is 8.5 MPa. This value is low compared to that obtained using clay only (

Table 2 **sample 3**: 24.1 MPa). The decrease in tensile strength is attributed to the increase of pores size and open porosity, in perfect agreement with the theoretical model described by Dean et al. [30].

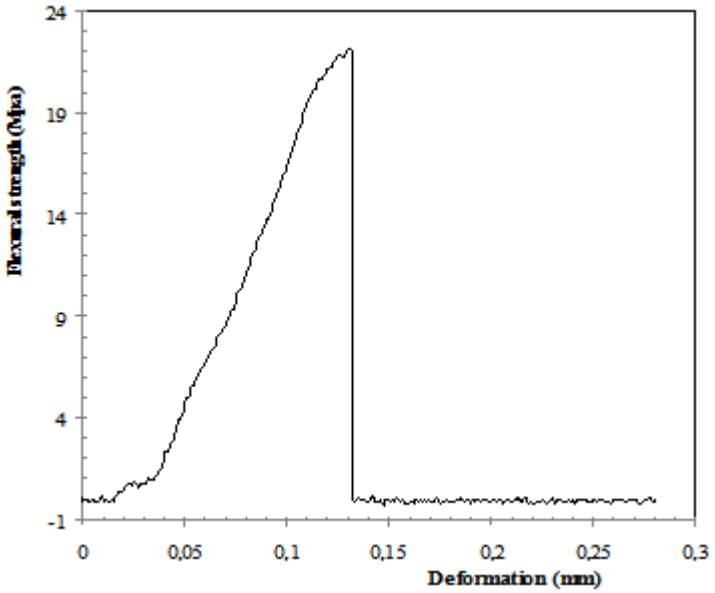

Figure 6: Typical flexural load– displacement curve of sintered samples

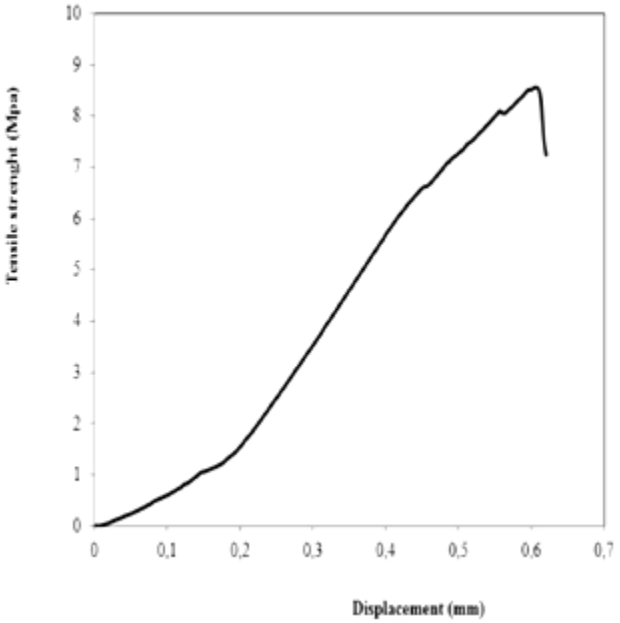

Figure 7: Typical load–displacement curve of sample 6 sintered at 1100 °C under diametral compression

The evolution of dynamic elastic properties determined by ultrasonic non-destructive testing of **sample 6** are summarized in

Table 4. The Young's modulus (E) and Poisson's ratio (ν) values obtained at 1100 °C are relatively higher than that reported in the literature for clay ceramics, namely by Lee and Yeh [31] and by Aston et al. [32].

Table 4: Elastic properties of sample 6 sintered at 1100°C

Property	**Value**
Apparent density ($g \cdot cm^{-3}$)	1.67
Longitudinal velocity ($m \cdot s^{-1}$)	3372
Transversal velocity ($m \cdot s^{-1}$)	2099
Young modulus E_D (GPa)	17.37
Shear modulus G (GPa)	7.34
Poisson ratio ν	0.18

IV. Conclusions

Within the framework of the development of Moroccan natural resources, we have carried out a study on Moroccan oil shales and raw clay in order to prepare new materials. The following conclusions can be drawn from the present investigation on the microstructural and mechanical characterizations of porous ceramics produced from both clay only and oil shales-clay mixtures:

- Macroporous ceramics with good mechanical properties can be prepared from 1:1 mixtures of oil shale and clay
- Material produced at 1100 °C was highly porous compared to other reported in the literature for clay ceramics formed at 1100 °C [23]. Open porosity > 40% with uniform pore diameter of 1.5–3 μm can be achieved. These results show that the use of oil shale as natural and less expensive pores forming agent can be an interesting alternative for the manufacture of porous ceramics.
- When increasing the firing temperature from 1000 to 1100 °C, an increase in the flexural strength and reduction in the porosity was observed for ceramics prepared from clay only. Conversely, in the case of oil shales/clay mixtures, both the porosity and mechanical properties increased.
- The Young's modulus and Poisson's ratio (ν) values obtained in this study at 1100 °C were higher than those reported for porous clay ceramics.

Acknowledgements

This work was financially supported by the Academy Hassan II of Science and Technology (Morocco), which are gratefully acknowledged. The authors thank the project leader
Professor Hannache, Hassan II University, Casablanca, Morocco

References

[1]. Nandi BK, Uppaluri R, Purkait MK. Preparation and characterization of low cost ceramic membranes for micro-filtration applications. App Clay Sci 2008;42:102–110.
[2]. Pagana AE, Sklari SD, Kikkinides ES, Zaspalis VT. Microporous ceramic membrane technology for the removal of arsenic and chromium ions from contaminated water. Microporous Mesoporous Mater 2008;110:150–156.
[3]. Cuperus FP, Nijhuis HH. Applications of membrane technology to food processing. Trends Food Sci 1993;4:277–286.
[4]. Sommer S, Melin T. Performance evaluation of microporous inorganic membranes in the dehydration of industrial solvents. Chem Eng Process 2005;44:1138–1156.
[5]. De Lange RSA, Hekkink JHA, Keizer K, Burggraaf AJ. Formation and characterization of supported microporous ceramic membrane prepared by sol-gel modification techniques. J Membrane Sci 1995;99:57–75.
[6]. Julbe A, Guizard C, Larbot A, Giroir-Fendler A. The sol-gel approach to prepare candidate microporous inorganic membranes for membrane reactors. J Membrane Sci 1993;77:137–153.
[7]. Meinema HA, Dirrix RWJ, Brinkman HW, Terpstra RA, Jerkele J, Kösters PH. Ceramic membranes for gas separation-recent developments and state of the art. Int Ceram 2005;54:86–91.
[8]. Sala B, Julbe A, Barboiu C, Cot D. Développement de membranes céramiques pour la separation de gaz à haute temperature. Patent Areva-NP/CNRS 2005 n° Fr 0513150.
[9]. Yang JL, Yu JL, Huang Y. Recent developments in gel casting of ceramics. J Eur Ceram Soc 31 (2011) 2569–2591.
[10]. Studart AR, Gonzenbach UT, Tervoort E, Gauckler LJ. Processing routes to macroporous ceramics: a review. J Amer Ceram Soc 89 (2006) 1771–1789.
[11]. Deng ZY, Fukasawa T, Ando M, Zhang GJ, Ohji T. High-surface-area alumina ceramics fabricated by the decomposition of $Al(OH)_3$. J Amer Ceram Soc 84 (2001) 485–491.
[12]. Gregorová E, Pabst W. Process control and optimized preparation of porous alumina ceramics by starch consolidation casting. J Eur Ceram Soc 31 (2011) 2073–2081.
[13]. Okada K, Shimizu M, Isobe T, Kameshima Y, Sakai M, Nakajima A, Kurata T. Characteristics of microbubbles generated by porous mullite ceramics prepared by an extrusion method using organic fibers as the pore former. J Eur Ceram Soc 2010;30:1245–1251.
[14]. Li S, Wang CA, Zhou J. Effect of starch addition on microstructure and properties of highly porous alumina ceramics. Ceram Int 2013;39:8833–8839.
[15]. Feng Y, Wang K, Yao J, Webley PA, Smart S, Wang H. Effect of the addition of polyvinylpyrrolidone as a pore-former on microstructure and mechanical strength of porous alumina ceramics. Ceram Int 2013;39:7551–7556.
[16]. Stoyanova DD, Vladov DCh, Kasabova NA, Mekhandzhiev DR. Cordierite-like catalyst supports based on clay materials. Kinetics Catal 2005;46:609–612.
[17]. Acimovic Z, Pavlovic L, Trumbulovic L, Andric L, Stamatovic M. Synthesis and characterization of the cordierite ceramics from non-standard raw materials for application in foundry. Mater Lett 2003;57:2651–2656.
[18]. Liu S, Zeng YP, Jiang D. Fabrication and characterization of cordierite-bonded porous SiC ceramics. Ceram Int 2009;35:597–602.
[19]. Saffaj N, Loukili H, Alami Younssi S, Albizane A, Bouhria M, Persin M, Larbot A. Filtration of solution containing heavy metals and dyes by means of ultrafiltration membranes deposited on support made of Moroccan clay. Desalination 2004;168:301–306.
[20]. Abourriche AK, Oumam M, Hannache H, Abourriche AM, Birot M, Pailler R, Naslain R. Contribution to the valorization of Moroccan oil shales. E-book "Green Energy & Technology" Bentham Science Publishers. Vol 1: pp.84–99 (2012)
[21]. Abourriche A, Oumam M, Hannache H, Pailler R, Naslain R, Birot M, Pillot JP. New pitches with very significant maturation degree obtained by supercritical extraction of Moroccan oil shales. J Supercrit Fluids 2008;47:195–199.
[22]. Benhammou A, El Hafiane Y, Abourriche A, Nibou L, Yaacoubi A, Tessier-Doyen N, Smith A, Tanouti B, Effects of oil shale addition and sintering cycle on the microstructure and mechanical properties of porous cordierite-ceramic, J Ceram Int 2014;40:8937–8944
[23]. Powder Diffraction File "Data sets 1–51 plus 70–89", ICDD, Release 2001.
[24]. Saffaj N, Persin M, Alami Younsi S, Albizane A, Cretin M, Larbot A. Elaboration and characterization of microfiltration and ultrafiltration membranes deposited on raw support prepared from natural Moroccan clay: Application to filtration of solution containing dyes and salts. App Clay Sci 2006;31:110–119.
[25]. Campbell JH. The kinetics of decomposition of Colorado oil shale: II: carbonate minerals UCRL52089, Part 2, 13 mars 1978.
[26]. El Moudden N, Elghazouali A, Rakib S, Sghyar M, Rafiq M, Larbot A, Cot L. Nouveaux supports membranaires à base de chamotte d'argile. Ann Chim 2001;26:5–1.
[27]. Rendtroff NM, Garrido LB, Aglietti EF. Mechanical and fracture properties of zircon-mullite composites obtained by direct sintering. Ceram Int 2009;35:2907–2913.
[28]. Rendtroff NM, Garrido LB, Aglietti EF. Effect of the addition of mullite-zirconia to the thermal shock behavior of zircon materials. Mater Sci Eng A, 2008;498:208–215.
[29]. Soro NS. Ph.D. Thesis, Limoges University, France, 2003.
[30]. Dean EA, Lopez JA, Empirical dependence of elastic moduli on porosity for ceramic materials, Journal of Am Cer Soc 1983;66:366–370.
[31]. Lee VG, Yeh TH. Sintering effects on the development of mechanical properties of fired clay ceramics. Mater Sci Eng A 2008;485:5–13.
[32]. Aston SD, Challis RE, Yiasemides GP. The dependence of the elastic properties of silica/alumina materials on the conditions used for firing, J Eur Ceram Soc 2002;22:1119–1127.